INFECTION AND IMMUNITY, July 2009, p. 2762–2772 Vol. 77, No. 7
0019-9567/09/$08.00+0 doi:10.1128/IAI.00323-09

Urothelial Cultures Support Intracellular Bacterial Community Formation by Uropathogenic *Escherichia coli*[▽]

Ruth E. Berry, David J. Klumpp,* and Anthony J. Schaeffer

Department of Urology, Feinberg School of Medicine, Northwestern University, 303 East Chicago Avenue, Chicago, Illinois 60611

Received 20 March 2009/Returned for modification 29 April 2009/Accepted 4 May 2009

Uropathogenic *Escherichia coli* (UPEC) causes most community-acquired and nosocomial urinary tract infections (UTI). In a mouse model of UTI, UPEC invades superficial bladder cells and proliferates rapidly, forming biofilm-like structures called intracellular bacterial communities (IBCs). Using a gentamicin protection assay and fluorescence microscopy, we developed an in vitro model for studying UPEC proliferation within immortalized human urothelial cells. By pharmacologic manipulation of urothelial cells with the cholesterol-sequestering drug filipin, numbers of intracellular UPEC CFU increased 8 h and 24 h postinfection relative to untreated cultures. Enhanced UPEC intracellular proliferation required that the urothelial cells, but not the bacteria, be filipin treated prior to infection. However, neither UPEC frequency of invasion nor early intracellular trafficking events to a Lamp1-positive compartment were modulated by filipin. Upon inspection by fluorescence microscopy, cultures with enhanced UPEC intracellular proliferation exhibited large, dense bacterial aggregates within cells that resembled IBCs but were contained with Lamp1-positive vacuoles. While an isogenic *fimH* mutant was capable of forming these IBC-like structures, the mutant formed significantly fewer than wild-type UPEC. Similar to IBCs, expression of *E. coli* iron acquisition systems was upregulated by intracellular UPEC. Expression of other putative virulence factors, including *hlyA*, *cnf1*, *fliC*, *kpsD*, and the biofilm adhesin *yfaL* also increased, while expression of *fimA* decreased and that of *flu* did not change. These results indicate that UPEC differentially regulates virulence factors in the intracellular environment. Thus, immortalized urothelial cultures that recapitulate IBC formation in vitro represent a novel system for the molecular and biochemical characterization of the UPEC intracellular life cycle.

Urinary tract infections (UTI) are the second most common infectious disease, in which uropathogenic *Escherichia coli* (UPEC) causes approximately 80% of community-acquired infections and 40% of nosocomial infections (51, 62, 63). UTI result in seven million clinic visits per year and cost $3.5 billion in treatment, representing a significant burden on the health care system (37). Half of all women will suffer a UTI during their lifetime, with a 25% recurrence rate within 6 months (10, 15). In 50% of these recurrent infections, the same UPEC strain causes both the primary and relapsing UTI (16, 25).

Several host-pathogen interactions between urothelial cells and UPEC have been characterized, including UPEC induction of apoptosis, suppression of cytokine secretion, and invasion of urothelial cells (3, 4, 9, 11, 30, 31, 38, 40, 61). UPEC invasion can be mediated by the Dr adhesin, which binds type IV collagen and decay-accelerating factor, or by type 1 pili, which binds mannose residues by the FimH adhesin. Invasion by either mechanism can result in a persistent infection (18, 19, 41, 43, 44, 56, 57). When type 1 pilus-expressing UPEC is internalized, UPEC proliferates and differentiates into intracellular bacterial communities (IBCs), compact aggregates of intracellular bacteria with biofilm-like properties that have been characterized in a murine UTI model (1, 26, 71). IBCs are primarily identified visually by their morphology and location. IBCs are globular in shape, are tightly packed with coccoid bacteria, and typically occupy most of the host cell cytoplasm, causing urothelial cell distortion. Formation occurs 6 to 24 h postinfection, and IBCs express antigen 43 and type 1 pili and secrete a polysaccharide matrix (1, 26). Bacterial genes *leuX*, *fimH*, and *surA* are required for IBC formation, and several iron acquisition systems are upregulated in IBCs (22, 26, 48, 71). Similar to the murine model, IBC-like structures have been identified during human UTIs. Exfoliated cells exhibiting features resembling IBCs were found in patient urine samples, and UPEC isolates originating from asymptomic bacteriura, pyelonephritis, and cystitis patients formed IBCs in the murine UTI model (17, 52).

Replicating the conditions required for IBC formation in vitro has proven to be difficult. One report described formation of IBC-like structures in a bladder carcinoma cell line after host cell permeabilization with a detergent (12). The absence of in vitro models is potentially due to the lack of cell lines that sufficiently recapitulate urothelial characteristics. Here we establish an in vitro model of IBC formation by pharmacologic manipulation of immortalized human urothelial cells. Our immortalized cell lines retain numerous characteristics of urothelial cells, including differentiation, inflammatory response, and apoptosis (3, 4, 30, 31, 39, 49, 64, 65). The IBC-like structures reported here are visually and morphologically similar to IBCs formed in the murine UTI model, occur with comparable kinetics, and similarly upregulate iron acquisition systems. Additionally, IBC formation is attenuated in a UPEC mutant lacking *fimH*. Thus, we have developed a model for studying UPEC IBC formation in vitro.

* Corresponding author. Mailing address: Department of Urology, Feinberg School of Medicine, Northwestern University, 303 East Chicago Avenue, Chicago, IL 60611. Phone: (312) 908-1996. Fax: (312) 908-7275. E-mail: d-klumpp@northwestern.edu.

▽ Published ahead of print on 18 May 2009.

MATERIALS AND METHODS

Cell lines and bacteria. PD07i cells were previously derived from pediatric human bladder and immortalized by introduction of human papillomavirus type 16 E6E7 (31). PD07i cells were cultured in serum-free EpiLife medium (Invitrogen) and were used in experiments up to passage 25. Type 1 piliated NU14 and isogenic *fimH* mutant NU14-1 were grown for 48 h in Luria-Bertani broth at 37°C under static conditions (31, 34).

Bacterial infections. (i) Quantifying adherence and viable invasive bacteria. PD07i cells seeded into 24-well dishes were infected with bacteria (multiplicity of infection [MOI] of 10), centrifuged twice at 600 × *g* for 2.5 min to synchronize infection, and incubated for 2 h at 37°C and 5% CO_2. Cells were washed four times with phosphate-buffered saline (PBS), and to measure bacterial adherence, cells were lysed with 0.5% trypsin (Gibco)–0.1% Triton X-100 (Calbiochem) and plated onto LB agar. Bacterial invasion was measured using a gentamicin protection assay. After 2 h of infection, PD07i cells were incubated with 100 μg/ml gentamicin (Fisher Scientific) for 30 min, followed by washing, lysing, and bacterial plating as described above. Invasion was normalized to the number of adherent bacteria: (no. of invasive CFU/adherent CFU) × 100%.

(ii) Intracellular proliferation. After infection of PD07i cells with UPEC as described above, cells were incubated with 100 μg/ml gentamicin for 22 h. PD07i cells were then lysed and bacteria were plated onto agar as described above. Proliferation was quantified as change (fold) at 24 h relative to 2 h (CFU 24 h/CFU 2 h). In the time course experiment, PD07i cells were infected with NU14 as described above, gentamicin was applied, and intracellular bacteria were enumerated every 2 h for a total of 24 h.

(iii) Drug treatments. PD07i cells were pretreated with 1 μg/ml filipin III (Sigma) or 7.5 mg/ml methyl-β-cyclodextrin (MβCD; Sigma) for 1 h prior to bacterial infection. Drugs did not affect the viability or growth of *E. coli*. Each condition was measured in duplicate, and each experiment was performed at least three times.

Microscopy. (i) Bacterial stain for quantifying total invasive bacteria. PD07i cells seeded onto coverslips were infected with NU14 (MOI of 10) for 1.5 h at 37°C and 5% CO_2. To stain extracellular bacteria, cells were incubated with a biotinylated rabbit anti-*E. coli* antibody (Abcam) diluted 1:1,000 in EpiLife–10% goat serum (Gibco) for 30 min at 37°C and 5% CO_2. Because this first antibody incubation occurred while the plasma membrane was still intact, antibodies only interacted with extracellular bacteria. Samples were washed four times with PBS and fixed in paraformaldehyde-lysine-periodate (PLP) fixative solution. Samples were permeabilized with 0.1% Triton X-100 for 5 min, washed four times with PBS, and blocked (10% goat serum), followed by incubation with streptavidin-Alexa Fluor 594 (red) (Invitrogen) to label extracellular bacteria. Samples were then reprobed with the biotinylated rabbit anti-*E. coli* antibody, followed by incubation with anti-rabbit–Alexa Fluor 488 (green) (Invitrogen). Because these antibody incubations occur after fixation and cell permeabilization, both intracellular and extracellular bacteria were stained green. Urothelial nuclei were stained by incubation with 4′,6-diamidino-2-phenylindole (DAPI) diluted 1:1,000 for 1 min. All reagents were diluted in PBS–5% sucrose.

To quantify invasion, images of 50 random fields of each coverslip were acquired. The number of bacteria associated with urothelial cells was counted, and those bacteria that stained both red and green were scored as adherent extracellular bacteria, while those that stained only green were scored as intracellular bacteria. At least three coverslips per condition were examined, and invasion efficiency was calculated: (invasive bacteria/adherent + invasive bacteria) × 100%.

(ii) *E. coli*-Lamp1 costain. PD07i cells were infected with NU14, and extracellular bacteria were stained as described above with a goat anti-*E. coli* antibody (Abcam) diluted 1:1,000. Cells were fixed as described above and blocked (3% bovine serum albumin, 0.05% milk, 0.1% saponin) at 37°C, followed by incubation with donkey anti-goat–Alexa Fluor 350 (Invitrogen) diluted 1:250 to label extracellular bacteria blue. Samples were reprobed with the goat anti-*E. coli* antibody and rabbit anti-Lamp1 antibody (Abcam) in buffer (1% bovine serum albumin, 0.05% saponin) for 1 h, followed by incubation with donkey anti-goat–Alexa Fluor 488 and donkey anti-rabbit–Alexa Fluor 594 (Invitrogen) to stain all bacteria green and Lamp1 red. To quantify Lamp1 colocalization, 50 to 100 intracellular bacteria (stained green but not blue) were scored as being Lamp1 positive or Lamp1 negative. A bacterium was considered Lamp1 positive only if Lamp1 staining was in the same plane as, and continuous around, the bacterium.

(iii) *E. coli*–caveolin-1 costain. PD07i cells were infected with NU14 (MOI of 100) for 1 h, fixed as described above, and blocked with 10% donkey serum–0.1% saponin. Sample was incubated with rabbit anti-caveolin-1 (Abcam) and goat anti-*E. coli* for 1 h, followed by incubation with donkey anti-rabbit–Alexa Fluor 594 and chicken anti-goat–Alexa Fluor 488, labeling caveolin-1 red and *E. coli* green. PD07i cell nuclei were counterstained with DAPI.

(iv) Intracellular proliferation. To qualitatively examine intracellular proliferation, PD07i cells were infected with NU14 expressing green fluorescent protein (NU14-GFP; MOI of 100). After 2 h, gentamicin (100 μg/ml) was applied, and cells were incubated at 37°C and 5% CO_2 for 22 h. Extracellular bacteria were stained, samples were fixed, and urothelial nuclei were stained as described above. To quantitatively examine intracellular proliferation, cells were infected with NU14 (MOI of 10) ± filipin as described above. After the 22-h incubation with gentamicin, extra- and intracellular bacteria were differentiated either by antibody incubation, as described above, or with the intercalating dye SYTO 9 (Invitrogen). The staining method did not affect the experimental outcome (data not shown). To differentiate intracellular and extracellular bacteria with SYTO 9, cultures were incubated with goat anti-*E. coli* antibody prior to fixation to label extracellular bacteria only. Samples were then permeabilized with 0.1% saponin for 5 min at 25°C to reduce background staining of the urothelial cell by SYTO 9. (Even with this permabilization step, SYTO 9 still stained urothelial nucleoli, which were easily identifiable and differentiated from *E. coli*.) Samples were then incubated with SYTO 9 (1.5:1,000) for 15 min to stain all bacteria green and fixed with PLP solution for 30 min, followed by incubations with rabbit anti-goat–Alexa Fluor 594 to label extracellular bacteria red and DAPI to stain urothelial nuclei blue. One hundred cells containing intracellular bacteria were scored for having 1 to 5, 6 to 20, or >20 intracellular bacteria or containing IBC-like structures.

All microscopic samples were washed four times with PBS–5% sucrose between each step, all antibodies were diluted 1:500, and all steps were incubated rocking for 30 min at room temperature unless indicated otherwise. Samples were mounted with Prolong Antifade (Invitrogen). Images were acquired on a Leica DMIRE microscope using Volocity acquisition and deconvolution software (Improvision). Z stacks were acquired in 0.1-μm intervals at ×63 or ×100, and stacks were deconvolved (25 iterations, 95% confidence). Images represent all slices of the Z stack compressed into one two-dimensional image unless otherwise indicated. Figure 1B was acquired on a Nikon Eclipse E800.

(v) Electron microscopy. PD07i cells in 35-mm-diameter dishes were infected with NU14 for 2 h (MOI of 100) as described above and fixed in 2.5% glutaraldehyde–0.1 M cacodylate buffer overnight. Samples were rinsed in 0.1 M cacodylate buffer, incubated in 2% osmium for 2 h, and then rinsed with distilled water. Samples were stained with uranyl acetate, rinsed with distilled water, and dehydrated with ethanol. Samples were embedded in a 1:1 mixture of ethyl alcohol-resin (mixture of araldite and Epon 812) and then incubated in a 60°C oven overnight. Specimens were sectioned with a diamond knife and mounted onto grids for imaging on a JEOL 1220 electron microscope.

Real-time PCR with RNA harvested from intracellular NU14. PD07i cells were incubated with NU14 (MOI of 100) for 2 h, followed by addition of gentamicin (100 μg/ml) to the culture medium for 22 h. To isolate intracellular bacteria, infected cultures were washed twice with PBS, incubated with RLT buffer (Qiagen) for 2 min, and vortexed for 1 min, followed by centrifugation for 1 min at 16,000 × *g*. This method has been shown to yield high-quality RNA for highly sensitive assays such as microarray analysis (8). Bacterial pellets were washed with PBS, and bacterial RNA was purified using the GenElute bacterial RNA harvest kit (Sigma). cDNA was synthesized with the iScript cDNA synthesis kit (Bio-Rad), and real-time PCR was performed with IQ SYBR green SuperMix (Bio-Rad) according to the manufacturer's instructions. Each condition was analyzed in duplicate. Real-time PCR was performed on an MJ Research PTC-200 Peltier thermal cycler, and data were recorded by the Opticon Monitor 3 software. Change in mRNA levels was determined using the $2^{-\Delta\Delta C_T}$ method, with *gyrB* as an internal control (45). The primers used are listed in Table 2. Primers did not amplify any product from uninfected PD07i cultures processed as described above.

Statistical analyses. A two-tailed unpaired *t* test, one-way analysis of variance, and two-way analysis of variance statistical analyses were performed using Prism 4.0a software (Graphpad Software). Data were considered significantly different at $P < 0.05$.

RESULTS

Intracellular proliferation by UPEC. We previously found that the immortalized human bladder cell line PD07i recapitulates many aspects of UPEC-urothelial cell interactions characterized in vivo, including FimH-dependent apoptosis, inflammatory responses, and UPEC binding and invasion (3, 4,

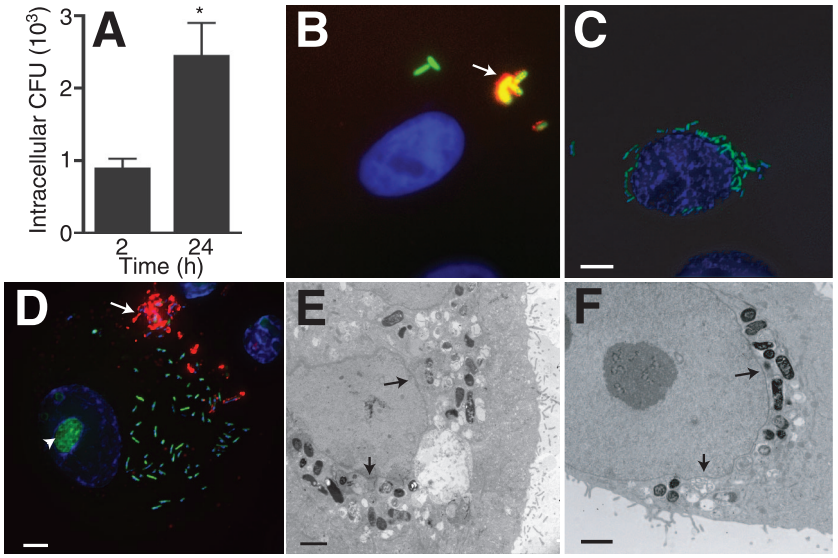

FIG. 1. NU14 proliferates within PD07i cells. (A) PD07i cells were infected with NU14 for 2 h, and intracellular bacteria were quantified by GPA after 2 h and 24 h of infection. *, $P < 0.01$ ($n = 10$). (B) PD07i cells were infected with NU14-GFP for 2 h and incubated with anti-*E. coli* antibody before fixation to stain extracellular bacteria only. Extracellular bacteria appear red/green (yellow), while intracellular bacteria appear green only. The sample was stained with DAPI to reveal the PD07i cell nucleus (blue). (C) Fluorescence microscopy of PD07i cells infected with NU14-GFP (green) for 24 h and stained with DAPI indicates proliferation of intracellular NU14 in the perinuclear region. (D) PD07i cells infected for 24 h and stained with SYTO 9 dye and DAPI show NU14 spread throughout the cytoplasm. Arrows, extracellular bacteria; arrowhead, PD07i cell nucleolus. Electron microscopy of PD07i cells infected with NU14 for 24 h shows that proliferating NU14 was spread throughout the cytoplasm (E) and in the perinuclear region (F). Arrows indicate nuclear membrane. Scale bars on immunofluorescence images are 5 μm, and scale bars on electron micrographs are 2 μm.

30, 31, 64, 65). To further explore UPEC-urothelial cell interactions, we tested the capacity of UPEC to proliferate within PD07i cells by gentamicin protection assay (GPA). PD07i cells were infected with the prototypical UPEC strain NU14 for 2 h, and then samples were incubated with gentamicin for 0.5 h to 22 h to kill extracellular bacteria, and detergent lysates were plated on agar to enumerate intracellular CFU. After 24 h, numbers of intracellular bacteria were significantly increased relative to numbers of intracellular bacteria after 2 h of infection (Fig. 1A) ($P < 0.01$). To determine if the increase in intracellular bacteria was due to intracellular proliferation, PD07i cells were incubated with NU14-GFP and then examined by immunofluorescence at 2 h and 24 h postinfection. To discriminate intracellular bacteria from extracellular bacteria, a dual staining was performed, whereby extracellular bacteria were first antibody stained prior to sample fixation and permeabilization so that the eukaryotic membrane protected intracellular bacteria from labeling. After 2 h of infection, intracellular NU14-GFP was rod shaped and distant from the host cell nucleus (Fig. 1B). PD07i cells contained 1.6 ± 0.5 invasive bacteria per cell, indicating that only 1 or 2 bacteria invaded each urothelial cell ($n = 5$). After 24 h, clusters of intracellular bacteria were identified within PD07i cells. Intracellular NU14-GFP appeared rod shaped, and clusters localized to the perinuclear space or were spread throughout the host cell cytoplasm (Fig. 1C and D). Examination of infected cells by electron microscopy showed similar distributions of intracellular bacteria after 24 h and suggested that the intracellular bacteria were membrane associated (Fig. 1E and F). To quantify NU14 intracellular proliferation, we counted the number of PD07i cells containing intracellular UPEC and classified these cells as containing 1 to 5, 6 to 20, or >20 bacteria/cell (Table 1). While nearly 80% of infected cells contained 1 to 5 bacteria after 24 h, 17.9% contained 6 to 20 bacteria, and 3.6% contained >20 bacteria. Together, these data suggest that NU14 proliferates within PD07i cells.

Filipin enhances UPEC intracellular proliferation. Cholesterol and lipid rafts have previously been implicated in UPEC invasion (9). We examined the role of lipid rafts in our PD07i model by using cholesterol-modifying drugs, including the cholesterol-sequestering agent filipin. When PD07i cultures were pretreated with filipin, the number of intracellular bacteria harvested after 24 h increased significantly relative to vehicle-treated PD07i cultures (Fig. 2A). Intracellular bacteria increased

TABLE 1. Quantification of intracellular proliferation by UPEC

Parameter	% of PD07i cells[a]:			
	NU14		NU14-1[b]	
	Control	Filipin	Control	Filipin
No. of bacteria/cell				
1–5	78.5 ± 3.2	82.4 ± 0.9	100 ± 0.0	97.3 ± 1.2
6–20	17.9 ± 3.8†	9.7 ± 1.6†	0 ± 0.0	0.7 ± 1.2
>20	3.6 ± 0.9	2.6 ± 0.6	0 ± 0.0	0 ± 0.0
IBCs	0 ± 0.0	5.2 ± 1.2**	0 ± 0.0	2.0 ± 0.02**
Total infected cells	19.8 ± 3.5	16.4 ± 1.0	1.2 ± 0.2*	2.1 ± 0.2*

[a] UPEC intracellular proliferation was determined by surveying 50 to 100 PD07i cells containing intracellular bacteria and quantifying the number of cells containing 1 to 5 bacteria, 6 to 20 bacteria, >20 bacteria, or IBCs after vehicle control or filipin pretreatment. *, $P < 0.05$; **, $P < 0.05$; †, $P < 0.05$.

[b] NU14-1 is an isogenic *fimH* mutant.

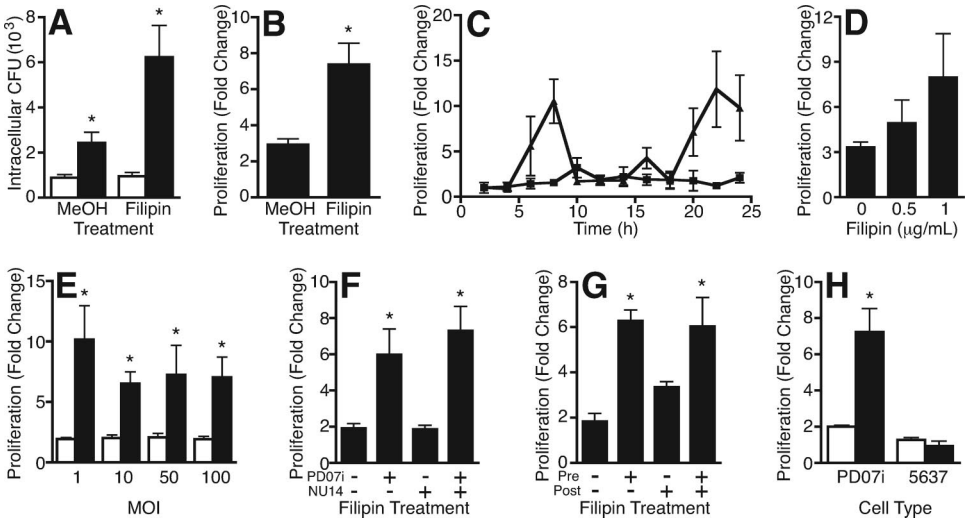

FIG. 2. Filipin enhanced intracellular proliferation of UPEC. (A) PD07i cells were infected with NU14 (MOI of 10), and the number of invasive CFU was measured after 2 h (white bars) and 24 h (black bars) by GPA. Intracellular CFU increased after 24 h of infection relative to 2 h of infection of vehicle control-pretreated (MeOH) or filipin-pretreated (1 μg/ml) PD07i cells. *, $P < 0.001$ ($n = 9$). (B) Proliferation over 24 h was calculated as change (fold) relative to 2 h (24 h CFU/2 h CFU). Intracellular proliferation significantly increased when PD07i cells were pretreated with filipin. *, $P = 0.002$ ($n = 9$). (C) Time course of NU14 intracellular proliferation within vehicle control-pretreated (squares) or filipin-pretreated (triangles) PD07i cells showed that filipin increased intracellular proliferation at 8 h and 24 h (representative experiment, $n = 2$). (D) PD07i cells were pretreated with different doses of filipin and then infected with NU14 for 2 h. Filipin-induced proliferation was dose dependent ($n = 3$). (E) Vehicle control-pretreated (white bars) or filipin-pretreated (black bars) PD07i cells were infected with NU14 at different MOIs. Filipin induced intracellular proliferation equally over an MOI range. *, $P < 0.001$ ($n = 3$). (F) PD07i cells or NU14 culture was pretreated with vehicle control (−) or filipin (+) prior to infection. Pretreatment of NU14 with filipin did not increase intracellular proliferation. *, $P < 0.05$ ($n = 5$). (G) PD07i cells were treated with vehicle control (−) or filipin (+) before (Pre) or after (Post) 2 h of NU14 infection. Filipin-induced proliferation occurred when PD07i cells were filipin treated preinfection but not postinfection. *, $P < 0.01$ ($n = 6$). (H) NU14 proliferation within PD07i cells or 5637 cells was similar to that in vehicle control-pretreated cells (white bars). Filipin pretreatment (black bars) induced proliferation in PD07i cells but not in 5637 cells. *, $P < 0.001$ ($n = 3$). Values depict the means of independent experiments ± the standard errors of the mean.

threefold over 24 h in vehicle-treated cells, while intracellular bacteria increased almost eightfold in filipin-pretreated PD07i cells, indicating that filipin enhanced NU14 intracellular proliferation (Fig. 2B). This effect was specific to filipin, for no difference in proliferation was seen when PD07i cultures were treated with other cholesterol-modifying drugs, including MβCD and nystatin (data not shown). This fortuitous finding led us to speculate whether the proliferation of intracellular UPEC had been altered.

To determine if filipin affected the morphology or distribution of proliferating intracellular bacteria, PD07i cultures were pretreated with filipin, infected with NU14-GFP, and then examined by fluorescence microscopy. At 24 h, intracellular NU14-GFP within filipin-pretreated PD07i cells appeared morphologically distinct from intracellular bacteria within untreated cells (compare Fig. 1C and D to 3A and B). Bacteria within vehicle-treated cells, which were indistinguishable from bacteria within untreated cells, appeared as loosely associated clusters, while bacteria within filipin-treated cells were packed together into globular, dense aggregates sufficiently sizeable to occupy large areas of the cell volume. These aggregates were often so large as to distort the nucleus itself. While filipin pretreatment did not affect the overall number of infected PD07i cells, filipin induced formation of these globular, dense aggregates in 5.2% of infected cells and significantly decreased the percentage of infected cells containing 6 to 20 bacteria (Table 1). Additionally, urothelial cells harboring these dense aggregates contained more bacteria per cell than vehicle-treated PD07i cells and were morphologically similar to the cytosolic IBCs reported in the murine UTI model (1, 26, 71). To determine if in vitro IBC-like structures are also cytosolic, samples were examined by electron microscopy. Imaging by electron microscopy confirmed the observed change in NU14 intracellular distribution and also suggested that these dense, globular aggregates were membrane bound (Fig. 3C). When samples were stained with the endosomal/lysosomal marker Lamp1, the IBC-like structures were surrounded by Lamp1 stain, suggesting containment within a Lamp1 vacuole (Fig. 3D). Thus, while in vitro IBC-like structures are morphologically similar to in vivo IBCs, they localize to a different compartment within urothelial cells.

Having identified IBC-inducing conditions in vitro, we sought to investigate the kinetics of the system and identify the system component modified by filipin. To this end, formation of IBC-like structures was characterized by a time course, a filipin dose curve, and an NU14 MOI curve. When the formation of IBC-like structures was characterized in a 24-h time course, two incidences of enhanced intracellular proliferation were observed: the first 6 to 8 h postinfection and the second 22 to 24 h postinfection (Fig. 2C). These data suggest that IBC-like structures appear with similar kinetics to in vivo IBCs (26). Filipin-enhanced intracellular proliferation increased as the filipin concentration increased and remained consistent over a range of bacterial MOIs (Fig. 2D and E). These data indicate that filipin induces proliferation independent of infecting dose of bacteria with similar kinetics to the in vivo UTI

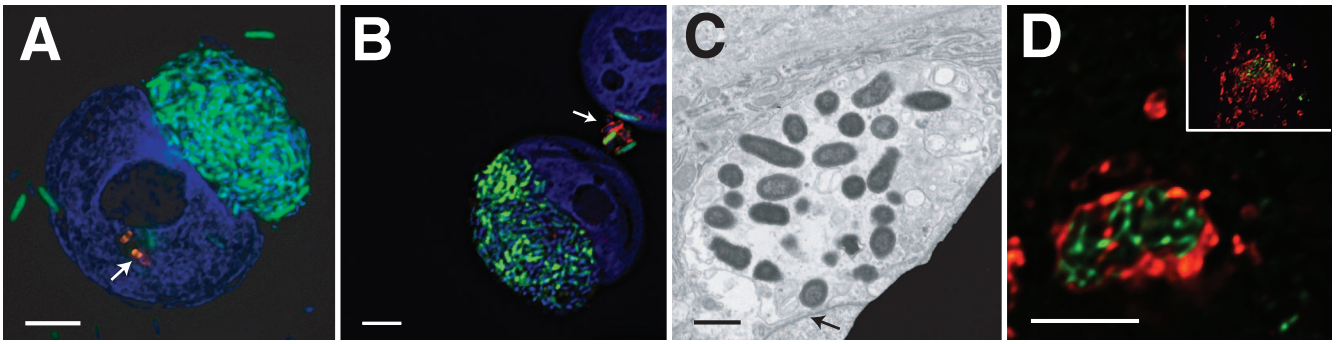

FIG. 3. Location and morphology of intracellular NU14. (A and B) Fluorescence image of PD07i cells pretreated with filipin and then infected with NU14-GFP (green) for 24 h. Cells were incubated with anti-*E. coli* antibody to stain extracellular bacteria (red) and with DAPI to indicate the urothelial cell nucleus (blue). Arrows indicate extracellular bacteria. (C) Electron micrograph of PD07i cells pretreated with filipin then infected with NU14 for 24 h suggested proliferating bacteria within a vacuole. An arrow indicates the cell nucleus. (D) PD07i cells pretreated with filipin and infected with NU14 for 24 h were stained with antibodies to Lamp1 (red) and to *E. coli* (green). The image represents one slice of a Z stack, and the inset represents the entire Z stack. Scale bars on immunofluorescence images are 5 μm, and scale bars on electron micrographs are 2 μm.

model. Although pretreatment of PD07i cultures enhanced NU14 intracellular proliferation, it was unclear whether filipin was acting on urothelial cells or on UPEC. Thus, to clarify where filipin was having an effect, either PD07i cultures or NU14 culture was treated with filipin prior to infection and NU14 intracellular proliferation was measured by GPA (Fig. 2F). As previously shown, when PD07i cultures were pretreated with filipin, intracellular bacterial proliferation was significantly higher than intracellular proliferation in vehicle-treated cultures ($P < 0.05$). Conversely, when NU14 was treated with filipin and then used to infect PD07i cultures, proliferation did not change. When both PD07i cells and bacteria were pretreated with filipin, proliferation was significantly increased over that of the control ($P < 0.01$). These data indicate that filipin acts on urothelial cultures, not the bacteria, to induce formation of IBC-like structures.

We next addressed whether the timing of filipin treatment influenced the formation of IBC-like structures. To this end, PD07i cells were treated with filipin either for 1 h prior to or for 1 h after NU14 infection. As previously seen, pretreatment of PD07i cells resulted in significantly higher NU14 intracellular proliferation relative to the vehicle-treated cultures (Fig. 2G). Treatment of cells postinfection slightly enhanced proliferation; however, this increase was not significantly different from vehicle-treated cultures. We also investigated whether IBC-like structures could be induced in another bladder cell line. The 5637 cell line is a bladder carcinoma cell line commonly used to study UPEC pathogenesis in vitro, yet filipin did not increase NU14 proliferation within 5637 cells (Fig. 2H). These data suggest that filipin acts on urothelial cells prior to bacterial infection to induce cellular changes that support enhanced UPEC proliferation and that not all urothelial cells are competent to support enhanced intracellular growth.

Filipin does not affect NU14 invasion of PD07i cells. Because filipin pretreatment was required, it was possible that filipin altered bacterial invasion, thereby leading to an alternative intracellular fate and IBC formation. To explore this possibility, PD07i cultures were pretreated with filipin, and NU14 invasion was measured by GPA and normalized to bacterial adherence. Pretreatment of PD07i cells with filipin had no effect on NU14 adherence or invasion efficiency (Fig. 4A) (data not shown). Filipin is a cholesterol-binding agent often used to disrupt lipid rafts, and the observation that filipin does not affect NU14 invasion contradicts previous reports suggesting that lipid rafts and caveolae are required for FimH-expressing *E. coli* to invade bladder cells (9). To investigate whether UPEC uses caveolae to invade PD07i cells, lipid rafts were disrupted with the cholesterol-extracting drug MβCD prior to NU14 infection. MβCD treatment resulted in decreased invasion efficiency compared to treatment with the vehicle control (Fig. 4B). To corroborate the GPA results, invasion was quantified by microscopy (Fig. 4C). MβCD pretreatment resulted in decreased NU14 invasion ($P < 0.05$), while filipin pretreatment did not affect invasion, confirming that cholesterol and lipid rafts were required for invasion. As further verification that caveolae mediate UPEC invasion, PD07i cells were stained for *E. coli* and for caveolae. In both vehicle-treated and filipin-treated cultures, NU14 localized to caveolae (Fig. 4E and F). Additionally, knocking down caveolin-1 by RNA interference resulted in significantly decreased NU14 invasion, suggesting that caveolae mediate NU14 invasion in PD07i cultures (data not shown). We also examined NU14 early intracellular trafficking events and found that after 2 h, 43% of intracellular NU14 colocalized with host endosomal/lysosomal marker Lamp1 (Fig. 4G). We quantified Lamp1 colocalization after filipin pretreatment and found that there was no significant difference relative to vehicle-treated samples (Fig. 4D). Together, these data suggest that filipin does not disrupt invasion or Lamp1 association to induce in vitro IBCs.

Role of FimH in IBC formation in vitro. Previous reports suggest that FimH is required for IBC formation (71). To determine if in vitro IBC-like structures require FimH, PD07i cultures were infected with the *fimH* mutant NU14-1, and adherence, invasion, and intracellular proliferation were measured by GPA. NU14-1 was significantly deficient for adherence compared to NU14, and NU14-1 adherence was not influenced by filipin (Fig. 5A). We next quantified invasion by NU14-1. While previous studies report that UPEC invasion requires FimH, we found that invasive NU14-1 was detectable

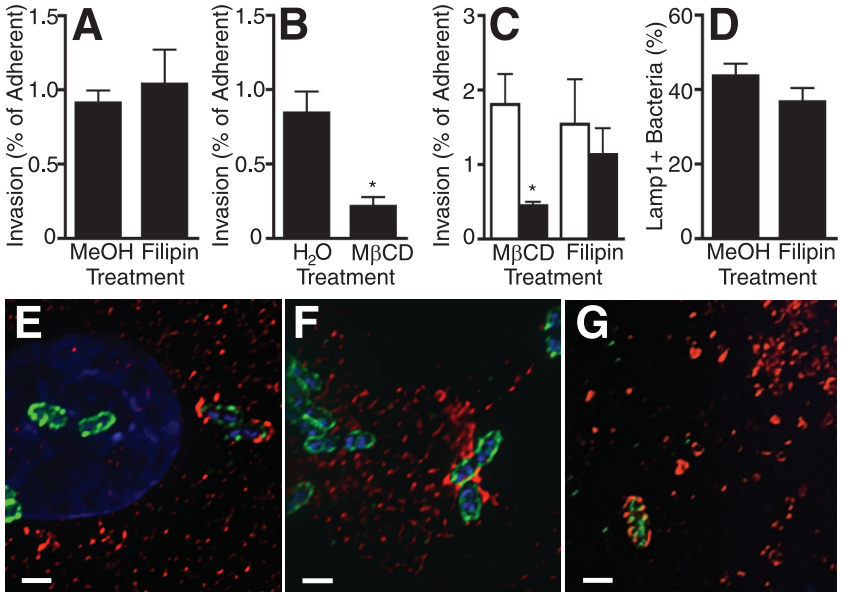

FIG. 4. Filipin does not affect NU14 invasion of PD07i cells. (A) PD07i cells were pretreated with a vehicle control (MeOH) or filipin (1 μg/ml) and then infected with NU14 (MOI of 10) for 2 h. Invasion was measured by GPA and expressed as a percentage of adherent bacteria. Filipin had no effect on invasion ($n = 10$), but pretreatment with MβCD (7.5 mg/ml) (B) significantly inhibited NU14 invasion (*, $P = 0.007$; $n = 4$). (C) PD07i cells were infected with NU14 as described above after pretreatment with the vehicle control (white bars) or the indicated drug (black bars), and invasion was measured by fluorescence microscopy of samples stained for extracellular and total bacteria as described in Materials and Methods. Invasion was significantly inhibited by MβCD but not filipin. *, $P < 0.05$ ($n = 4$). (D) PD07i cells were pretreated and infected as described above and then stained for Lamp1, extracellular bacteria, and total bacteria. Association of intracellular NU14 with Lamp1 was quantified and was unaffected by filipin pretreatment ($n = 3$). Fluorescence microscopy of PD07i cells infected 1 h with NU14 and stained with DAPI (blue), anti-*E. coli* antibody (green), and anti-caveolin-1 antibody (red) shows that NU14 localized to caveolin-1 in vehicle control-pretreated (E) and filipin-pretreated (F) PD07i cells. (G) Fluorescence microscopy of PD07i cells infected for 2 h with NU14 and stained with anti-*E. coli* antibody (green) and Lamp1 antibody (red) shows NU14 within a Lamp1$^+$ compartment. Scale bars are 1 μm. Values depict the means of independent experiments ± standard errors of the mean.

by both GPA and by immunofluorescence at an MOI of 100 and that NU14-1 invasion increased significantly with filipin pretreatment. ($P < 0.05$) (Fig. 5B and D). To determine if NU14-1 was subject to filipin-enhanced proliferation, intracellular bacteria were quantified 24 h postinfection by GPA. We found that filipin significantly increased the number of intracellular NU14-1 CFU and induced IBC-like structures (Fig. 5C and E). The number of bacteria/cell was enumerated to quantify intracellular proliferation, and in vehicle-treated cultures, all cells containing intracellular NU14-1 had fewer than five bacteria per cell, indicating that NU14-1 cannot proliferate within PD07i cells (Table 1). Under IBC-inducing conditions, IBC-like structures appeared in 2% of infected cells; however, NU14-1 formed significantly fewer in vitro IBCs than NU14 ($P < 0.01$). These data suggest that *fimH* is not absolutely necessary for invasion but is required for intracellular proliferation, a requirement that is partially relieved under IBC-inducing conditions.

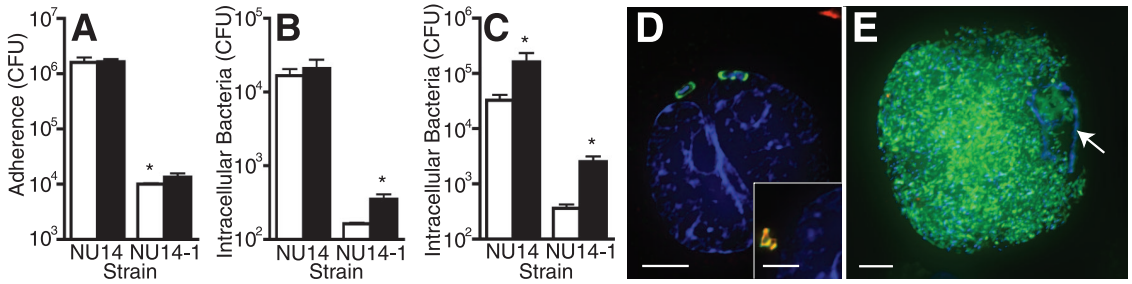

FIG. 5. Role of FimH during in vitro IBC formation. (A) PD07i cells were pretreated with vehicle control (white bars) or filipin (black bars) and infected for 2 h with the indicated strain (MOI of 100), and bacterial adherence was measured by colony counts of cell lysates plated on LB agar. *, $P < 0.0001$. (B) PD07i cells were pretreated with vehicle control or filipin and infected with bacteria for 2 h, and invasive bacteria were quantified by GPA. Filipin significantly increased invasion by NU14-1. *, $P < 0.05$. (C) PD07i cells were treated with filipin and incubated with bacteria, and after 24 h, intracellular CFU were quantified by GPA. Filipin significantly increased the number of intracellular NU14 and NU14-1 CFU. *, $P < 0.05$. (D) Immunofluorescence image of a PD07i cell infected with NU14-1 for 24 h and dually stained to differentiate intracellular (green) and extracellular bacteria (red and green; inset image), and counterstained with DAPI (blue; PD07i cell nuclei). (E) Immunofluorescence image of a filipin-treated PD07i cell infected with NU14-1 for 24 h and dually stained to identify intracellular bacteria (SYTO 9 labeled; green) and with DAPI to label the PD07i cell nucleus (blue; arrow). Scale bars are 5 μm. Values depict the means of independent experiments ± standard errors of the means.

TABLE 2. Primers for measuring bacterial gene expression

Gene (UTI89 identification no.)	Putative role in UTIs	Protein function	Primer	Source or reference
chuA (C4028)	Iron acquisition	Heme utilization transport protein	Forward, 5′ AAGGCGTTGCCCAATACCAGAGTA 3′ Reverse, 5′ TATTCCGATCGCTCACAGTGGCTT 3′	48, 60
fepA (C0584)	Iron acquisition	Ferric enterobactin receptor	Forward, 5′ ACGTTCAATCATTTCAGGCGGCAC 3′ Reverse, 5′ TCAGCGTGGTAATAACCGCCAGAT 3′	6, 48, 60
iroN (C1118)	Iron acquisition	Salmochelin siderophore receptor	Forward, 5′ ACCGGAACAGGTTGAGCGTATTGA 3′ Reverse, 5′ TGGTGTATAACGACAGCGAACCGT 3′	48, 60
sitA (C1339)	Iron acquisition	AB-type ferric iron transport system	Forward, 5′ TGGTGACCATCCATCGCTGATTCT 3′ Reverse, 5′ TACGATCCGGCAAATGCACAAACC 3′	48, 60
entF (C0588)	Iron acquisition	Enterobactin synthetase F	Forward, 5′ TCAGGTGTGCAGCGTACCGATTTA 3′ Reverse, 5′ CCGCAATGTGAATACCCAATGGCA 3′	6, 48, 60
tonB (C1451)	Iron acquisition	Energy transduction	Forward, 5′ GGTCTGCATTCATGGTGCTGTTGT 3′ Reverse, 5′ CAACCATCGTGACAGAAATCGGCT 3′	48, 60
ybtS (C2178)	Iron acquisition	Putative salicylate synthetase	Forward, 5′ GCAAACAGCCTCCAGTTCAGCAAT 3′ Reverse, 5′ TGGTGATGTCAGTGACGGGCAATA 3′	48
fliC (C2124)	Motility	Flagellar filament protein	Forward, 5′ GCGCTTTCGACATGTTGGACACTT 3′ Reverse, 5′ AATTCCGTTCTTCCCTGGGTGCTA 3′	60
fimA (C5011)	Cell adhesion	Major type 1 subunit fimbrin	Forward, 5′ CTGGCAATTGTTGTTCTGTCGGCT 3′ Reverse, 5′ AACGGTTTGATCAACAGAGCCTGC 3′	1, 60
flu (C1139)	Biofilm formation	Antigen 43	Forward, 5′ TAACAGCGTCCGTCTCAGCATTCA 3′ Reverse, 5′ AACATCAACGGAAGAATGGCCTGC 3′	1, 60, 68
yfaL (C2514)	Biofilm formation	Putative adhesion	Forward, 5′ TAATTCGCTGTCGAGCAGTAGCGT 3′ Reverse, 5′ TGACGCTGGCAGGTGAGCTTAATA 3′	6
kpsD (C3364)	K capsule	Polysialic acid transport protein	Forward, 5′ AGTCAGCTAAATGCCCTGGTCACA 3′ Reverse, 5′ AATCAGACGTCACACCGCCATACA 3′	55, 60
hlyA (C4926)	Pore-forming toxin	α-Hemolysin	Forward, 5′ TCACGAATTTCCTCACCGGGAGTT 3′ Reverse, 5′ TTATGAAGAGGGAAAGCGGCTGGA 3′	48, 59, 70
cnf1 (C4921)	GTPase deamidase	Cytotoxic nectrotizing factor; toxin	Forward, 5′ ATGCAGCAAGCAGACGACACTTTC 3′ Reverse, 5′ ATATCAGGAGGCGTTGATGGCTCA 3′	7, 47, 59
gyrB (C4249)	NA[a]	Gyrase	Forward, 5′ CACTTTCACGGAAACGACCGCAAT 3′ Reverse, 5′ TTACCAACAACATTCCGCAGCGTG 3′	

[a] NA, not applicable.

In vitro IBCs upregulate expression of iron acquisition systems. Because IBCs are mainly identified by morphology, there are no definitive markers for confirming that the globular, dense aggregates observed in our in vitro model are IBCs. However, expression of several genes involved in iron acquisition was measured and the genes were found to be upregulated in mouse IBCs (48). To further characterize in vitro IBCs, we measured gene expression of several iron acquisition systems under IBC-inducing and noninducing conditions. Thus, PD07i cultures were pretreated with vehicle control or filipin and infected with NU14 for 24 h. Intracellular bacteria were isolated, bacterial RNA was purified, and real-time reverse transcription-PCR (RT-PCR) was performed on 15 potential virulence factors (Table 2) (8). Gene expression of intracellular bacteria was normalized to that of bacteria grown in PD07i culture medium under static conditions.

We examined the expression of genes involved in several iron acquisition systems that are upregulated in IBCs: *chuA*, *fepA*, *iroN*, *sitA*, *entF*, *tonB*, and *ybtS* (Fig. 6A to G and Table 2) (48). These genes have been reported by multiple groups to be important for UPEC pathogenesis in vivo, so expression in vitro would be indicative of a model that closely mimics in vivo events (6, 21). We found that under IBC-inducing conditions, expression of *fepA*, *iroN*, *entF*, *tonB*, and *ybtS* was significantly elevated compared to static growth conditions, while expression of *sitA* remained unchanged (Fig. 6A to G, compare condition M to condition F). *chuA* expression was elevated, but expression was not significantly higher under IBC-inducing conditions than in culture medium. With the exception of *sitA*, our in vitro IBCs show the same trend in expression of iron acquisition systems as IBCs within mouse bladders. Notably, the same changes in gene expression were observed under

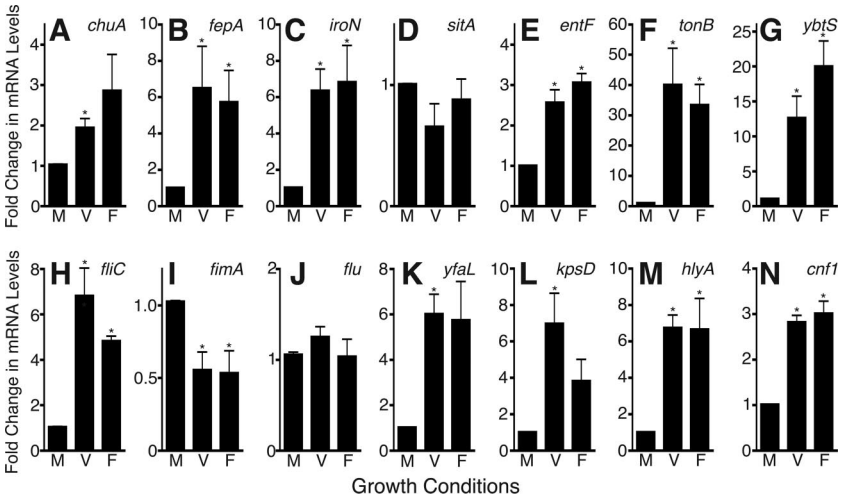

FIG. 6. In vitro IBCs upregulate expression of putative UPEC virulence factors. PD07i cells were pretreated with the vehicle control (V) or filipin (F) and then infected with NU14 (MOI of 100) for 2 h followed by addition of gentamicin to the culture medium for 22 h. Bacteria were isolated from PD07i cells, and bacterial RNA was harvested as detailed in Materials and Methods. RNA was also prepared from NU14 grown in culture medium (M) under static conditions for 24 h. Each condition was performed in duplicate, and each RNA sample was assayed in duplicate using the $2^{-\Delta\Delta CT}$ method. Values were normalized to *gyrB* mRNA levels and are expressed as change (fold) from gene expression in culture medium. Graphs represent the means of three experiments ± standard errors of the mean. *, $P < 0.05$. (A to G) Genes involved in iron acquisition. (H to N) Putative UPEC virulence factors. See Table 2 for gene details.

noninducing conditions, suggesting that the urothelial intracellular environment is sufficient to alter UPEC gene expression (see Discussion).

We also measured the expression of several other virulence factors proposed to play a role in UPEC pathogenesis, including *fliC*, *fimA*, *flu*, *yfaL*, *kpsD*, *hlyA*, and *cnf1* (Table 2). *hlyA*, which is upregulated in mouse IBCs, was also significantly upregulated under IBC-inducing conditions (Fig. 6M) (20, 58, 59, 67, 70). *fliC* is downregulated in mouse urine but upregulated during growth in human urine and was upregulated under intracellular conditions in our model (Fig. 6H) (60). Expression of other putative virulence factors, including *yfaL*, *cnf1*, and *kpsD*, was also upregulated by the intracellular environment, yet *kpsD* expression increased significantly only under noninducing conditions. *fimA*, coding for the major subunit of type 1 pili, was downregulated relative to expression in culture medium (Fig. 6I, K, L, and N) (1, 60, 71). However, overall expression remained relatively high as *fimA* expression in culture medium was 10-fold higher than that of the internal control, *gyrB* (data not shown). *flu* expression remained constant between culture medium and intracellular conditions, corroborating observations that antibodies to antigen 43 react with both extracellular and intracellular UPEC (Fig. 6J) (1, 60, 68; data not shown). Thus, other virulence factor genes exhibited changes in expression associated with the PD07i intracellular environment.

DISCUSSION

UPEC undergoes extensive intracellular proliferation within mouse bladder cells to form cytosolic, biofilm-like IBCs by 6 to 24 h postinfection. In the murine UTI model, IBCs embed in a secreted polysaccharide, express antigen 43 and type 1 pili, require bacterial genes *fimH*, *leuX*, and *surA*, and upregulate iron acquisition systems (1, 22, 26–28, 41, 42, 48, 71). Using light microscopy, immunofluorescence, and electron microscopy, similar IBCs were identified in human urine samples by morphology and intracellular location (52). Using a gentamicin protection assay, immunofluorescence, and electron microscopy, we identified in vitro conditions whereby large dense aggregates with IBC morphology form within immortalized human urothelial cells (Table 3). Similar to in vivo IBCs, in vitro IBCs form 6 to 24 h postinfection, upregulate iron acquisition systems, and express antigen 43. However, in contrast to in vivo IBCs that appear cytosolic (1), in vitro IBCs are contained in a Lamp1 compartment. Nonetheless, our in vitro IBC model shares many characteristics with in vivo IBCs, suggesting that this system will be useful for identifying host and bacterial factors required for IBC formation.

We also investigated the requirement for *fimH* in UPEC invasion and IBC formation in vitro. Previous reports state that FimH is required for UPEC invasion, yet very low levels of invasion, proliferation, and IBC formation by a *fimH* mutant have been documented (38, 71). We found the *fimH* mutant

TABLE 3. Comparison of in vivo and in vitro IBCs

IBC characteristic	Characteristic present:	
	In vivo	In vitro
Forms as dense aggregate of coccoid bacteria	Yes	Yes
Is cytosolic	Yes	No
Forms 6–24 h postinfection	Yes	Yes
Secretes polysaccharide	Yes	NT[a]
Stains for antigen 43	Yes	Yes
Is deficient as *fimH* mutant	Yes	Yes[b]
Requires *leuX* and *surA*	Yes	NT
Upregulates iron acquisition systems	Yes	Yes

[a] NT, not tested.
[b] The *fimH* mutant formed IBCs, but significantly fewer than wild-type UPEC.

NU14-1 invaded but did not proliferate within urothelial cells under basal conditions (Fig. 5C and Table 1). When grown under IBC-inducing conditions, however, NU14-1 formed IBCs, albeit less frequently (Table 1). These data suggest that intact type 1 pili are not required for IBC formation but instead influence the frequency with which IBCs form. We also found that under IBC-inducing conditions, NU14-1 invasion increased significantly (twofold) (Fig. 5B). These data suggest that IBC-inducing conditions enhance a *fimH*-independent invasion mechanism that targets bacteria to an alternative intracellular niche that is permissive for IBC formation. Identification of bacterial and host receptors responsible for enhanced NU14-1 invasion will help identify conditions under which IBCs are established and bacterial mechanisms of IBC formation.

We examined gene expression of virulence factors and compared expression profiles of intracellular bacteria to those of bacteria grown in culture medium (Table 2). There was a general increase in expression between medium and intracellular environments, but only *kpsD* expression was different between noninducing and IBC-inducing conditions (Fig. 6). Registad et al. compared iron acquisition gene expression by IBCs, which are intracellular by definition, to gene expression in extracellular bacteria obtained from culture medium or intestine (48). No comparison between IBCs and intracellular but non-IBC bacteria was possible, so while genes were upregulated in IBCs relative to extracellular environments, expression patterns were not necessarily IBC specific. Our studies were also limited in that only 5.2% of cells containing bacteria had IBC structures (Table 1), so gene induction under IBC-inducing conditions may be masked by the presence of non-IBC intracellular bacteria. However, since the NU14 contained within in vitro IBCs outnumber intracellular NU14 underbasal conditions approximately threefold (Fig. 2B), quantitative RT-PCR data likely reflect IBC gene expression. Based upon these considerations, our data suggest that upregulation of iron acquisition systems and other virulence factors are not specific to IBCs but are characteristic of intracellular UPEC, consistent with other intracellular pathogens (13, 46).

In measuring gene expression of virulence factors, we found intracellular UPEC downregulated *fimA*; upregulated *fliC*, *kpsD*, *yfaL*, *cnf1*, and *hlyA*; and did not alter *flu* expression (Fig. 6). Decreased *fimA* expression may reflect a reduced need for lengthy type 1 pili within the limited intracellular space. Since type 1 pilus expression represses flagellar expression, decreased expression of the *fim* operon likely derepresses *fliC*, resulting in increased *fliC* expression by intracellular bacteria (33). K1 capsule masks bacterial surface structures, which helps decrease detection by immune surveillance, decrease phagocytosis, and modulate trafficking of *E. coli*-containing vacuoles (29, 50, 53, 69). Thus, increased *kpsD* expression could help direct UPEC intracellular trafficking and avoid lysosomal degradation. Alternatively, antigen 43 function is blocked by both K1 capsule and type 1 pili (23, 53). The combination of decreased *fim* expression and the drop in *kpsD* expression under IBC-inducing conditions compared to basal conditions may permit antigen 43-mediated autoaggregation, thus facilitating biofilm and IBC formation. Cnf1 inactivates GTPases, which has multiple effects on the cell, including actin reorganization (5, 7, 14, 32, 35, 36, 54, 59). A previous report suggests that UPEC intracellular proliferation is restricted by actin structure, so *cnf1* upregulation may disrupt the actin network, facilitating UPEC intracellular growth (12). Overall, virulence factor gene expression patterns of in vitro IBCs support and extend previous observations and suggest testable hypotheses for the UPEC intracellular life cycle.

IBC-inducing conditions required urothelial cell pretreatment with filipin, indicating that host cell modification prior to infection facilitates IBC formation. In vitro IBC formation within a Lamp1 vacuole suggests that filipin modifies subcellular compartments to permit IBC formation. These compartments likely have nearly identical conditions to umbrella cells that support IBC formation, and examination of host changes that have occurred in these compartments will help identify cellular environments permissive to IBC formation. Although filipin modifies cholesterol, cholesterol is not the sole factor mediating IBC formation, as other cholesterol-modifying drugs do not have this effect. Others have also reported that MβCD and filipin have differential effects. In a model of B-cell signaling, MβCD fully disrupted lipid rafts while filipin left them only partially disrupted (2). Filipin could exert differential effects on specific domains within the urothelial cell plasma membrane, perhaps leaving some lipid rafts intact, such as caveolae that mediate invasion, while disrupting others. Other groups have observed that Toll-like receptor 4 (TLR4) knockout mice form more IBC than wild-type mice and that TLR4 knockdown urothelial cultures exhibited increased UPEC invasion (61). TLR4 agonist promote receptor translocation to lipid rafts, and filipin can abrogate TLR4-mediated signaling (24, 66). Thus, we speculate that filipin differentially disrupts urothelial lipid rafts, such as TLR4-containing rafts, but leaves caveolae intact, thereby leading to the enhanced *fimH*-independent invasion and subsequent IBC formation. Alternatively, filipin also decreases adenylate cyclase activity and cyclic AMP (cAMP) levels, and an adenylate cyclase-3-dependent pathway was recently described that mediates cAMP-dependent fluxing of *E. coli* out of urothelial cells (61). Therefore, filipin-induced decreases in cAMP could promote *fimH*-independent invasion and retention, thus shifting the equilibrium toward IBC formation. Future experiments will resolve these competing models.

In summary, here we present a model of UPEC IBC formation in urothelial cultures. IBCs formed in vitro are morphologically comparable to in vivo IBCs and share many physical characteristics. This model will facilitate biochemical and genetic studies of host and pathogen requirements for IBC formation and UPEC pathogenesis. Finally, this system will accelerate the identification and testing of novel therapeutics for eradication of IBCs in the treatment and prevention of UTIs.

ACKNOWLEDGMENTS

This work was supported by the Alumnae of Northwestern University (R.E.B.) and NIH awards R01 DK04628 (A.J.S.) and T32 AI007476 (R.E.B.).

We thank Lennell Reynolds for assistance with electron microscopy. We also thank Ben Billips, Praveen Thumbikat, and Ryan Yaggie for useful discussions. We thank Charles Rudick for critical review of the manuscript.

REFERENCES

1. **Anderson, G. G., J. J. Palermo, J. D. Schilling, R. Roth, J. Heuser, and S. J. Hultgren.** 2003. Intracellular bacterial biofilm-like pods in urinary tract infections. Science **301:**105–107.
2. **Awasthi-Kalia, M., P. P. Schnetkamp, and J. P. Deans.** 2001. Differential effects of filipin and methyl-beta-cyclodextrin on B cell receptor signaling. Biochem. Biophys. Res. Commun. **287:**77–82.
3. **Billips, B. K., S. G. Forrestal, M. T. Rycyk, J. R. Johnson, D. J. Klumpp, and A. J. Schaeffer.** 2007. Modulation of host innate immune response in the bladder by uropathogenic *Escherichia coli*. Infect. Immun. **75:**5353–5360.
4. **Billips, B. K., A. J. Schaeffer, and D. J. Klumpp.** 2008. Molecular basis of uropathogenic *Escherichia coli* evasion of the innate immune response in the bladder. Infect. Immun. **76:**3891–3900.
5. **Bower, J. M., D. S. Eto, and M. A. Mulvey.** 2005. Covert operations of uropathogenic Escherichia coli within the urinary tract. Traffic **6:**18–31.
6. **Chen, S. L., C. S. Hung, J. Xu, C. S. Reigstad, V. Magrini, A. Sabo, D. Blasiar, T. Bieri, R. R. Meyer, P. Ozersky, J. R. Armstrong, R. S. Fulton, J. P. Latreille, J. Spieth, T. M. Hooton, E. R. Mardis, S. J. Hultgren, and J. I. Gordon.** 2006. Identification of genes subject to positive selection in uropathogenic strains of Escherichia coli: a comparative genomics approach. Proc. Natl. Acad. Sci. USA **103:**5977–5982.
7. **Davis, J. M., H. M. Carvalho, S. B. Rasmussen, and A. D. O'Brien.** 2006. Cytotoxic necrotizing factor type 1 delivered by outer membrane vesicles of uropathogenic *Escherichia coli* attenuates polymorphonuclear leukocyte antimicrobial activity and chemotaxis. Infect. Immun. **74:**4401–4408.
8. **Di Cello, F., Y. Xie, M. Paul-Satyaseela, and K. S. Kim.** 2005. Approaches to bacterial RNA isolation and purification for microarray analysis of *Escherichia coli* K1 interaction with human brain microvascular endothelial cells. J. Clin. Microbiol. **43:**4197–4199.
9. **Duncan, M. J., G. Li, J. S. Shin, J. L. Carson, and S. N. Abraham.** 2004. Bacterial penetration of bladder epithelium through lipid rafts. J. Biol. Chem. **279:**18944–18951.
10. **Engel, J. D., and A. J. Schaeffer.** 1998. Evaluation of and antimicrobial therapy for recurrent urinary tract infections in women. Urol. Clin. N. Am. **25:**685–701, x.
11. **Eto, D. S., T. A. Jones, J. L. Sundsbak, and M. A. Mulvey.** 2007. Integrin-mediated host cell invasion by type 1-piliated uropathogenic Escherichia coli. PLoS Pathog. **3:**e100.
12. **Eto, D. S., J. L. Sundsbak, and M. A. Mulvey.** 2006. Actin-gated intracellular growth and resurgence of uropathogenic Escherichia coli. Cell. Microbiol. **8:**704–717.
13. **Fischbach, M. A., H. Lin, D. R. Liu, and C. T. Walsh.** 2006. How pathogenic bacteria evade mammalian sabotage in the battle for iron. Nat. Chem. Biol. **2:**132–138.
14. **Flatau, G., E. Lemichez, M. Gauthier, P. Chardin, S. Paris, C. Fiorentini, and P. Boquet.** 1997. Toxin-induced activation of the G protein p21 Rho by deamidation of glutamine. Nature **387:**729–733.
15. **Foxman, B., B. Gillespie, J. Koopman, L. Zhang, K. Palin, P. Tallman, J. V. Marsh, S. Spear, J. D. Sobel, M. J. Marty, and C. F. Marrs.** 2000. Risk factors for second urinary tract infection among college women. Am. J. Epidemiol. **151:**1194–1205.
16. **Foxman, B., L. Zhang, P. Tallman, K. Palin, C. Rode, C. Bloch, B. Gillespie, and C. F. Marrs.** 1995. Virulence characteristics of Escherichia coli causing first urinary tract infection predict risk of second infection. J. Infect. Dis. **172:**1536–1541.
17. **Garofalo, C. K., T. M. Hooton, S. M. Martin, W. E. Stamm, J. J. Palermo, J. I. Gordon, and S. J. Hultgren.** 2007. *Escherichia coli* from urine of female patients with urinary tract infections is competent for intracellular bacterial community formation. Infect. Immun. **75:**52–60.
18. **Goluszko, P., S. L. Moseley, L. D. Truong, A. Kaul, J. R. Williford, R. Selvarangan, S. Nowicki, and B. Nowicki.** 1997. Development of experimental model of chronic pyelonephritis with Escherichia coli O75:K5:H-bearing Dr fimbriae: mutation in the dra region prevented tubulointerstitial nephritis. J. Clin. Investig. **99:**1662–1672.
19. **Goluszko, P., V. Popov, R. Selvarangan, S. Nowicki, T. Pham, and B. J. Nowicki.** 1997. Dr fimbriae operon of uropathogenic Escherichia coli mediate microtubule-dependent invasion to the HeLa epithelial cell line. J. Infect. Dis. **176:**158–167.
20. **Gurcel, L., L. Abrami, S. Girardin, J. Tschopp, and F. G. van der Goot.** 2006. Caspase-1 activation of lipid metabolic pathways in response to bacterial pore-forming toxins promotes cell survival. Cell **126:**1135–1145.
21. **Hagan, E. C., and H. L. T. Mobley.** 2007. Uropathogenic *Escherichia coli* outer membrane antigens expressed during urinary tract infection. Infect. Immun. **75:**3941–3949.
22. **Hannan, T. J., I. U. Mysorekar, S. L. Chen, J. N. Walker, J. M. Jones, J. S. Pinkner, S. J. Hultgren, and P. C. Seed.** 2008. LeuX tRNA-dependent and -independent mechanisms of Escherichia coli pathogenesis in acute cystitis. Mol. Microbiol. **67:**116–128.
23. **Hasman, H., T. Chakraborty, and P. Klemm.** 1999. Antigen-43-mediated autoaggregation of *Escherichia coli* is blocked by fimbriation. J. Bacteriol. **181:**4834–4841.
24. **Hornef, M. W., B. H. Normark, A. Vandewalle, and S. Normark.** 2003. Intracellular recognition of lipopolysaccharide by toll-like receptor 4 in intestinal epithelial cells. J. Exp. Med. **198:**1225–1235.
25. **Ikaheimo, R., A. Siitonen, T. Heiskanen, U. Karkkainen, P. Kuosmanen, P. Lipponen, and P. H. Makela.** 1996. Recurrence of urinary tract infection in a primary care setting: analysis of a 1-year follow-up of 179 women. Clin. Infect. Dis. **22:**91–99.
26. **Justice, S. S., C. Hung, J. A. Theriot, D. A. Fletcher, G. G. Anderson, M. J. Footer, and S. J. Hultgren.** 2004. Differentiation and developmental pathways of uropathogenic Escherichia coli in urinary tract pathogenesis. Proc. Natl. Acad. Sci. USA **101:**1333–1338.
27. **Justice, S. S., S. R. Lauer, S. J. Hultgren, and D. A. Hunstad.** 2006. Maturation of intracellular Escherichia coli communities requires SurA. Infect. Immun. **74:**4793–4800.
28. **Kerrn, M. B., C. Struve, J. Blom, N. Frimodt-Moller, and K. A. Krogfelt.** 2005. Intracellular persistence of Escherichia coli in urinary bladders from mecillinam-treated mice. J. Antimicrob. Chemother. **55:**383–386.
29. **Kim, K. J., S. J. Elliott, F. Di Cello, M. F. Stins, and K. S. Kim.** 2003. The K1 capsule modulates trafficking of E. coli-containing vacuoles and enhances intracellular bacterial survival in human brain microvascular endothelial cells. Cell. Microbiol. **5:**245–252.
30. **Klumpp, D. J., M. T. Rycyk, M. C. Chen, P. Thumbikat, S. Sengupta, and A. J. Schaeffer.** 2006. Uropathogenic *Escherichia coli* induces extrinsic and intrinsic cascades to initiate urothelial apoptosis. Infect. Immun. **74:**5106–5113.
31. **Klumpp, D. J., A. C. Weiser, S. Sengupta, S. G. Forrestal, R. A. Batler, and A. J. Schaeffer.** 2001. Uropathogenic *Escherichia coli* potentiates type 1 pilus-induced apoptosis by suppressing NF-κB. Infect. Immun. **69:**6689–6695.
32. **Kouokam, J. C., S. N. Wai, M. Fällman, U. Dobrindt, J. Hacker, and B. E. Uhlin.** 2006. Active cytotoxic necrotizing factor 1 associated with outer membrane vesicles from uropathogenic *Escherichia coli*. Infect. Immun. **74:**2022–2030.
33. **Lane, M. C., A. N. Simms, and H. L. T. Mobley.** 2007. complex interplay between type 1 fimbrial expression and flagellum-mediated motility of uropathogenic *Escherichia coli*. J. Bacteriol. **189:**5523–5533.
34. **Langermann, S., S. Palaszynski, M. Barnhart, G. Auguste, J. S. Pinkner, J. Burlein, P. Barren, S. Koenig, S. Leath, C. H. Jones, and S. J. Hultgren.** 1997. Prevention of mucosal Escherichia coli infection by FimH-adhesin-based systemic vaccination. Science **276:**607–611.
35. **Lerm, M., G. Schmidt, U. M. Goehring, J. Schirmer, and K. Aktories.** 1999. Identification of the region of rho involved in substrate recognition by Escherichia coli cytotoxic necrotizing factor 1 (CNF1). J. Biol. Chem. **274:**28999–29004.
36. **Lerm, M., J. Selzer, A. Hoffmeyer, U. R. Rapp, K. Aktories, and G. Schmidt.** 1999. Deamidation of Cdc42 and Rac by *Escherichia coli* cytotoxic necrotizing factor 1: activation of c-Jun N-terminal kinase in HeLa cells. Infect. Immun. **67:**496–503.
37. **Litwin, M. S., and C. S. Siagal.** 2007. Introduction, p. 3–7. *In* M. S. Litwin and C. S. Siagal (ed.), Urologic diseases in America. NIH publication no. 07-5512. Department of Health and Human Services, Washington, DC.
38. **Martinez, J. J., M. A. Mulvey, J. D. Schilling, J. S. Pinkner, and S. J. Hultgren.** 2000. Type 1 pilus-mediated bacterial invasion of bladder epithelial cells. EMBO J. **19:**2803–2812.
39. **Mudge, C. S., and D. J. Klumpp.** 2005. Induction of the urothelial differentiation program in the absence of stromal cues. J. Urol. **174:**380–385.
40. **Mulvey, M. A., Y. S. Lopez-Boado, C. L. Wilson, R. Roth, W. C. Parks, J. Heuser, and S. J. Hultgren.** 1998. Induction and evasion of host defenses by type 1-piliated uropathogenic Escherichia coli. Science **282:**1494–1497.
41. **Mulvey, M. A., J. D. Schilling, and S. J. Hultgren.** 2001. Establishment of a persistent *Escherichia coli* reservoir during the acute phase of a bladder infection. Infect. Immun. **69:**4572–4579.
42. **Mysorekar, I. U., and S. J. Hultgren.** 2006. Mechanisms of uropathogenic Escherichia coli persistence and eradication from the urinary tract. Proc. Natl. Acad. Sci. USA **103:**14170–14175.
43. **Nowicki, B., A. Labigne, S. Moseley, R. Hull, S. Hull, and J. Moulds.** 1990. The Dr hemagglutinin, afimbrial adhesins AFA-I and AFA-III, and F1845 fimbriae of uropathogenic and diarrhea-associated *Escherichia coli* belong to a family of hemagglutinins with Dr receptor recognition. Infect. Immun. **58:**279–281.
44. **Nowicki, B., R. Selvarangan, and S. Nowicki.** 2001. Family of Escherichia coli Dr adhesins: decay-accelerating factor receptor recognition and invasiveness. J. Infect. Dis. **183**(Suppl. 1)**:**S24–S27.
45. **Parsons, D. A., and F. Heffron.** 2005. *sciS*, an *icmF* homolog in *Salmonella enterica* serovar Typhimurium, limits intracellular replication and decreases virulence. Infect. Immun. **73:**4338–4345.
46. **Radtke, A. L., and M. X. O'Riordan.** 2006. Intracellular innate resistance to bacterial pathogens. Cell. Microbiol. **8:**1720–1729.
47. **Real, J. M., P. Munro, C. Buisson-Touati, E. Lemichez, P. Boquet, and L. Landraud.** 2007. Specificity of immunomodulator secretion in urinary samples in response to infection by alpha-hemolysin and CNF1 bearing uropathogenic Escherichia coli. Cytokine **37:**22–25.

48. **Reigstad, C. S., S. J. Hultgren, and J. I. Gordon.** 2007. Functional genomic studies of uropathogenic Escherichia coli and host urothelial cells when intracellular bacterial communities are assembled. J. Biol. Chem. **282:**21259–21267.
49. **Rickard, A., N. Dorokhov, J. Ryerse, D. J. Klumpp, and J. McHowat.** 2008. Characterization of tight junction proteins in cultured human urothelial cells. In Vitro Cell. Dev. Biol. **44:**261–267.
50. **Roberts, I. S.** 1996. The biochemistry and genetics of capsular polysaccharide production in bacteria. Annu. Rev. Microbiol. **50:**285–315.
51. **Ronald, A.** 2003. The etiology of urinary tract infection: traditional and emerging pathogens. Dis. Mon. **49:**71–82.
52. **Rosen, D. A., T. M. Hooton, W. E. Stamm, P. A. Humphrey, and S. J. Hultgren.** 2007. Detection of intracellular bacterial communities in human urinary tract infection. PLoS Med. **4:**e329.
53. **Schembri, M. A., D. Dalsgaard, and P. Klemm.** 2004. Capsule shields the function of short bacterial adhesins. J. Bacteriol. **186:**1249–1257.
54. **Schmidt, G., P. Sehr, M. Wilm, J. Selzer, M. Mann, and K. Aktories.** 1997. Gln 63 of Rho is deamidated by Escherichia coli cytotoxic necrotizing factor-1. Nature **387:**725–729.
55. **Schwan, W. R., M. T. Beck, S. J. Hultgren, J. Pinkner, N. L. Woolever, and T. Larson.** 2005. Down-regulation of the *kps* region 1 capsular assembly operon following attachment of *Escherichia coli* type 1 fimbriae to D-mannose receptors. Infect. Immun. **73:**1226–1231.
56. **Selvarangan, R., P. Goluszko, V. Popov, J. Singhal, T. Pham, D. M. Lublin, S. Nowicki, and B. Nowicki.** 2000. Role of decay-accelerating factor domains and anchorage in internalization of Dr-fimbriated *Escherichia coli*. Infect. Immun. **68:**1391–1399.
57. **Selvarangan, R., P. Goluszko, J. Singhal, C. Carnoy, S. Moseley, B. Hudson, S. Nowicki, and B. Nowicki.** 2004. Interaction of Dr adhesin with collagen type IV is a critical step in *Escherichia coli* renal persistence. Infect. Immun. **72:**4827–4835.
58. **Smith, Y. C., K. K. Grande, S. B. Rasmussen, and A. D. O'Brien.** 2006. Novel three-dimensional organoid model for evaluation of the interaction of uropathogenic *Escherichia coli* with terminally differentiated human urothelial cells. Infect. Immun. **74:**750–757.
59. **Smith, Y. C., S. B. Rasmussen, K. K. Grande, R. M. Conran, and A. D. O'Brien.** 2008. Hemolysin of uropathogenic *Escherichia coli* evokes extensive shedding of the uroepithelium and hemorrhage in bladder tissue within the first 24 hours after intraurethral inoculation of mice. Infect. Immun. **76:**2978–2990.
60. **Snyder, J. A., B. J. Haugen, E. L. Buckles, C. V. Lockatell, D. E. Johnson, M. S. Donnenberg, R. A. Welch, and H. L. Mobley.** 2004. Transcriptome of uropathogenic *Escherichia coli* during urinary tract infection. Infect. Immun. **72:**6373–6381.
61. **Song, J., B. L. Bishop, G. Li, M. J. Duncan, and S. N. Abraham.** 2007. TLR4 initiated and cAMP mediated abrogation of bacterial invasion of the bladder. Cell Host Microbe **1:**287–298.
62. **Stamm, W. E., and T. M. Hooton.** 1993. Management of urinary tract infections in adults. N. Engl. J. Med. **329:**1328–1334.
63. **Struelens, M. J., O. Denis, and H. Rodriguez-Villalobos.** 2004. Microbiology of nosocomial infections: progress and challenges. Microbes Infect. **6:**1043–1048.
64. **Thumbikat, P., R. E. Berry, B. K. Billips, R. E. Yaggie, G. Zhou, T. T. Sun, A. J. Schaeffer, and D. J. Klumpp.** 2009. Bacteria-induced uroplakin signaling mediates bladder response to infection. PLoS Pathog **5:**e1000415. doi: 1000410.1001371/journal.ppat.1000415.
65. **Thumbikat, P., R. E. Berry, A. J. Schaeffer, and D. J. Klumpp.** 2009. Differentiation-induced uroplakin III expression promotes urothelial cell death in response to uropathogenic E. coli. Microbes Infect. **11:**57–65.
66. **Triantafilou, M., S. Morath, A. Mackie, T. Hartung, and K. Triantafilou.** 2004. Lateral diffusion of Toll-like receptors reveals that they are transiently confined within lipid rafts on the plasma membrane. J. Cell Sci. **117:**4007–4014.
67. **Uhlen, P., A. Laestadius, T. Jahnukainen, T. Soderblom, F. Backhed, G. Celsi, H. Brismar, S. Normark, A. Aperia, and A. Richter-Dahlfors.** 2000. Alpha-haemolysin of uropathogenic E. coli induces Ca^{2+} oscillations in renal epithelial cells. Nature **405:**694–697.
68. **Ulett, G. C., J. Valle, C. Beloin, O. Sherlock, J.-M. Ghigo, and M. A. Schembri.** 2007. Functional analysis of antigen 43 in uropathogenic *Escherichia coli* reveals a role in long-term persistence in the urinary tract. Infect. Immun. **75:**3233–3244.
69. **Vermeulen, C., A. Cross, W. R. Byrne, and W. Zollinger.** 1988. Quantitative relationship between capsular content and killing of K1-encapsulated *Escherichia coli*. Infect. Immun. **56:**2723–2730.
70. **Wiles, T. J., B. K. Dhakal, D. S. Eto, and M. A. Mulvey.** 2008. Inactivation of host Akt/protein kinase B signaling by bacterial pore-forming toxins. Mol. Biol. Cell **19:**1427–1438.
71. **Wright, K. J., P. C. Seed, and S. J. Hultgren.** 2007. Development of intracellular bacterial communities of uropathogenic Escherichia coli depends on type 1 pili. Cell. Microbiol. **9:**2230–2241.

Editor: A. J. Bäumler